Tao, D., Feng, C., Lu, Y., Cui, Y., Yang, X., Manners, I., Winnik, M. A., & Huang, X. (2018). Self-seeding of block copolymers with a π-conjugated oligo(p-phenylene vinylene) segment: a versatile route toward monodisperse fiber-like nanostructures. *Macromolecules*, *51*(5), 2065-2075. https://doi.org/10.1021/acs.macromol.8b00046

Self-Seeding of Block Copolymers with a π-Conjugated Oligo(*p*-phenylene vinylene) Segment: A Versatile Route toward Monodisperse Fiber-like Nanostructures

Daliao Tao,[a] *Chun Feng*,[a,*] *Yijie Lu*,[b] *Yinan Cui*,[a] *Xian Yang*,[a] *Ian Manners*,[c] *Mitchell A. Winnik*,[b,*] *Xiaoyu Huang*[a,*]

[a] Key Laboratory of Synthetic and Self-Assembly Chemistry for Organic Functional Molecules, Shanghai Institute of Organic Chemistry, University of Chinese Academy of Sciences, Chinese Academy of Sciences, 345 Lingling Road, Shanghai 200032, People's Republic of China

[b] Department of Chemistry, University of Toronto, 80 St. George St, Toronto, Ontario M5S 3H6, Canada

[c] School of Chemistry, University of Bristol, Cantock's Close, Bristol BS8 1TS, United of Kingdom

* To whom correspondence should be addressed, E-mail: cfeng@mail.sioc.ac.cn (Tel: +86-21-54925506, Fax: +86-21-64166128), mwinnik@chem.utoronto.ca (Tel: +1-416-978-6495, Fax: +1-416-978-0541), xyhuang@mail.sioc.ac.cn (Tel: +86-21-54925310, Fax: +86-21-64166128).

Abstract

Three well-defined crystalline-coil diblock copolymers of oligo(*p*-phenylene vinylene)-*b*-poly(*N*-isopropyl acrylamide) (OPV_5-*b*-$PNIPAM_{18}$, OPV_5-*b*-$PNIPAM_{49}$ and OPV_5-*b*-$PNIPAM_{75}$, the subscripts represent the number of repeat units of each block) with the same crystallizable core-forming OPV segment but different corona-forming PNIPAM blocks of various chain lengths were synthesized. Their solution self-assembly behavior was examined in methanol, ethanol and isopropanol. Both the solvent and the length of the PNIPAM block were found to affect the self-assembly of the block copolymers. In methanol, OPV_5-*b*-$PNIPAM_{18}$ formed a mixture of fiber-like micelles of uniform width and complex two-dimensional platelet-like structures with fiber-like micelles protruding from the ends. In ethanol and in isopropanol, this polymer only formed long fiber-like micelles of uniform width. OPV_5-*b*-$PNIPAM_{49}$ formed long fiber-like micelles (several micrometers) of uniform width in all three solvents, but under the same self-assembly conditions, OPV_5-*b*-$PNIPAM_{75}$ only formed short fiber-like micelles with lengths of several hundred nanometers. We examined systematically the temperature-induced self-seeding behavior of all three block copolymers, exploring the influence of PNIPAM chain length, solvent, annealing time and concentration of copolymer. The most remarkable result of these experiments is our finding that fiber-like micelles of uniform length, with controlled lengths up to 1 μm can be easily prepared from all three block copolymers, even from OPV_5-*b*-$PNIPAM_{75}$ that formed only much shorter micelles under self-nucleated self-assembly. We also showed that the self-seeding strategy can be extended to other OPV-containing diblock copolymer such as

Commented [F1]: delete

OPV$_5$-*b*-poly(2-(diethylamino)ethyl methacrylate) for preparing monodisperse fiber-like micelles of controllable length. These results show that the self-seeding approach to crystallization-driven self-assembly can be a versatile route to prepare uniform fiber-like micelles with controllable lengths for OPV-containing block copolymers.

Keywords: fiber-like micelle, crystalline-coil copolymer, crystallization-driven self-assembly, self-seeding.

Introduction

Since the pioneering work on the self-assembly of amphiphilic block copolymers (BCPs) in aqueous solution by Eisenberg and co-workers,[1,2] the self-assembly of BCPs in a selective solvent has attracted increasing attention due to their capacity for the formation of a variety of hierarchical nano- and micro-structures with broad application prospects in nanoscience and nanomedicine.[3,4] Most experiments in this field focus on coil-coil BCPs, which self-assemble into micelles consisting of an amorphous core and a solvent-swollen corona. For coil-coil BCPs in polar solvents, the hydrophobic effect is the main driving force. The morphology of the micelles formed by coil-coil BCPS is usually determined by three parameters. These include the stretching of the core-forming segment, the repulsion within the chains of the micellar corona, and the interfacial free energy between the solvent and the micellar core.[5] Factors affecting these three parameters, such as composition and concentration of coil-coil BCPs, temperature, pH and solvent polarity, will influence the micellar morphologies.[1-6] Although various nanostructures with different morphologies and diverse functionalities have been obtained by self-assembly of coil-coil BCPs, the preparation of elongated fiber-like structures is still challenging due to the narrow composition window for their formation.[6] Therefore, the formation of uniform fiber-like micelle with control over length and composition remains a challenge for coil-coil BCPs.

Studies on the self-assembly of crystalline-coil BCPs with a crystallizable core-forming segment have shown that core crystallization tends to promote the formation of cylindrical micelles or platelet nanostructures. Examples include poly(ferrocenyldimethylsilane) (PFS),[7-16] poly(ferrocenyldiethylsilane),[17] poly(ferrocenydimethylgermane),[18,19] poly(ethylene oxide)

(PEO),[20,21] polyacrylonitrile,[22] poly(ε-caprolactone),[23-27] polylactide,[28-34] polythiophene (PTH),[35-37] poly(hedral oligomeric silsesquioxane) (POSS)[38,39] and polyethylene (PE)[40-47] as the crystallizable core-forming block. The term "crystallization-driven self-assembly" (CDSA) has been used to describe cases in which crystallization of the core-forming block dominates the self-assembly process. Significantly, for PFS-based BCPs, the exposed ends of the core of cylindrical micelles remain active toward the further epitaxial addition of PFS-containing BCP unimers. This behavior is analogous to that of a living covalent polymerization, and thus this process has been called "living CDSA". The living CDSA of PFS-containing BCPs enables the preparation of not only fiber-like micelles with controllable lengths and compositions, but other hierarchical ordered 1-D and 2-D nano- or microstructures and related hybrid composites with precise structural control.[7-16]

In 1966, Kovacs and Keller reported that a heating and cooling process called "self-seeding" could be used to prepare single crystals of PE and PEO homopolymers.[48] Lotz and Keller found that self-seeding could also be extended to BCPs with a crystallizable segment to form planar raft-like micelles in a solvent selective for the non-crystalline block.[20] Since the degree of the chain order (crystallinity) of polymer crystals depends on the crystallization rate during their formation, as well as on their thermal history, polymer crystals usually contain regions of different order in chain packing. In a self-seeding process, when polymer crystals are heated above their apparent dissolution/melting temperatures, the regions of polymer with the highest crystalline order survive, and the rest of the polymer crystals with lower crystallinity dissolve. Upon cooling, the surviving crystallites would act as nuclei to initiate the growth by deposition

of the dissolved polymer, leading to the formation of large polymer crystals. Since the growth rate is essentially identical for all seed nuclei, uniform single crystal are formed. Recent publications also show that self-seeding is a facile tool to generate uniform two-dimensional polymer crystals for further applications.[49-52]

In 2010, Qian *et al*. reported the extension of the self-seeding strategy to the preparation of cylindrical micelles of PI_{1000}-*b*-PFS_{50} (PI = polyisoprene, the subscripts represent the number of repeat units of each block) in decane.[7] They found that long cylindrical micelles of uniform length ranging from about 50 nm to 1.7 μm could be generated by annealing decane solutions of short seed micelle fragments at different temperatures, followed by cooling to room temperature.[8] Recent reports showed that the self-seeding route can be employed with other PFS-containing BCPs, and also with BCPs with a crystalline polythiophene core-forming block[36,37] or with a liquid-crystalline poly(2-(perfluorooctyl)ethyl methacrylate) (PFMA) core-forming domain[53] to prepare cylindrical micelles of controlled length and narrow length distribution.

Although the self-seeding strategy seems to be a facile technique to generate uniform fiber-like micelles for BCPs with a crystalline core-forming block, reports on other crystalline-coil BCPs are still rare.[7,8,36,37,53] This is probably because that the landscape for self-seeding of CDSA may be more complex than one initially thought. For example, we recently published a communication to report the generation of uniform fiber-like micelles of controlled lengths with a crystalline oligo(*p*-phenylene vinylene) (OPV) core-forming block by a self-seeding process.[54] Although self-seeding can be successfully applied to both PFS-based and

OPV-containing BCPs, we found that the packing mode of OPV within the core is very different from that of PFS segments. For the self-assembly of OPV-containing BCPs, it is supposed that the core is formed in a face-to-face stacking fashion, where the OPV segment can not fold due to its rigidity.[54,55] In contrast, for PFS-containing copolymers, core-forming PFS chains form the core with a large number of folds to increase the distance between the anchor points of the corona chains so as to minimize strong corona chain repulsion.[56,57]

To deepen our understanding of self-seeding for the preparation of uniform fiber-like micelles from OPV-based copolymers and expand the scope for application of the self-seeding process, we need more information about how the experimental conditions and the structure of copolymers affect their self-assembly behavior. To obtain this kind of information, we synthesized a series of crystalline-coil BCPs of OPV-*b*-poly(*N*-isopropyl acrylamide) (OPV-*b*-PNIPAM) with the same crystallizable OPV segment but corona-forming PNIPAM blocks of different chain lengths (Scheme 1). We first examined the influence of chain length of the corona-forming PNIPAM block and the solvent on the self-assembly. The structures formed were characterized by transmission electron microscopy (TEM), atomic force microscopy (AFM) and grazing incidence wide-angle X-ray scattering (GIWAXS). We then investigated systematically the factors that affect the self-seeding of OPV-*b*-PNIPAM BCPs, including the chain length of PNIPAM block, annealing time, solvent and copolymer concentration. Finally, we also attempted to extend the self-seeding protocol to OPV-*b*-poly(2-(diethylamino)ethyl methacrylate) (OPV-*b*-PDEAEMA) for preparing uniform fiber-like micelles with controlled length (Scheme 1).

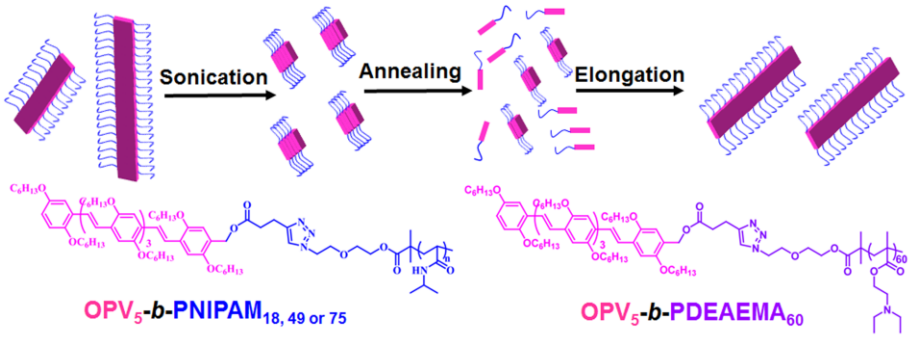

Scheme 1. Preparation of Uniform Fiber-like Micelles with an OPV Core by Self-seeding.

Results and Discussion

Synthesis of OPV-based Diblock Copolymers

We synthesized a series of OPV_5-*b*-$PNIPAM_{18}$, OPV_5-*b*-$PNIPAM_{49}$ and OPV_5-*b*-$PNIPAM_{75}$ diblock copolymers with the same OPV segment, but different PNIPAM chain lengths. Experimental details are presented in Supporting Information, SI. The synthetic procedure started with the preparation of an alkyne-terminated OPV_5 according to our previous report.[54] Then, a series of azide-terminated PNIPAM homopolymers with different chain lengths were prepared by atom radical transfer polymerization (ATRP) using an azide-containing initiator (Scheme S1).[58] The mono-azide end group functionality of PNIPAM homopolymer was confirmed by ^{1}H NMR (Figure S1). GPC measurements show that the molecular weights of azide-terminated PNIPAM homopolymers increased with a higher feed ratio of NIPAM monomer to initiator and with a longer polymerization time (Figure S2). All the azide-terminated PNIPAM homopolymer samples showed unimodal and symmetrical GPC eluent peaks with narrow molecular weight distributions ($M_w/M_n \leq 1.22$). Subsequently, the alkyne-terminated OPV_5 was coupled with each

azide-terminated PNIPAM homopolymer by the copper-catalyzed azide-alkyne cycloaddition (CuAAC) click reaction as described in Scheme S2.

The crude products obtained were purified by silica chromatography to remove unreacted OPV_5 and by washing with water to remove excess PNIPAM homopolymer. GPC analysis showed a shorter retention time of the purified product compared to that of each original PNIPAM homopolymer, indicative of the successful coupling between PNIPAM and OPV_5 (Figure S3). All OPV-*b*-PNIPAM diblock copolymers showed unimodal and symmetrical eluent peaks (both for RI and UV detectors) with narrow molecular weight distributions (Đ = 1.10, 1.10 and 1.23 for OPV_5-*b*-$PNIPAM_{18}$, OPV_5-*b*-$PNIPAM_{49}$ and OPV_5-*b*-$PNIPAM_{75}$, respectively, see Table 1). This observation indicates that unreacted PNIPAM and OPV were completely removed, and a possible intermolecular coupling reaction between PNIPAM with Br chain ends could be neglected. The chemical structure of OPV-*b*-PNIPAM was confirmed by ^{1}H NMR (Figure 1) and the molecular weights of OPV-*b*-PNIPAM samples were calculated on the basis of the predetermined M_n of OPV_5 and results from ^{1}H NMR analysis (Table 1).

Table 1. Characteristics of OPV-based Diblock Copolymers

Sample	M_n^{GPC} (g/mol)[a]	M_n^{NMR} (g/mol)[b]	Đ (GPC)[a]
OPV_5-*b*-$PNIPAM_{18}$	4700	3900	1.10
OPV_5-*b*-$PNIPAM_{49}$	7700	7400	1.10
OPV_5-*b*-$PNIPAM_{75}$	11200	10400	1.23
OPV_5-*b*-$PDEAEMA_{60}$	7900	13000	1.16

[a] Determined by GPC analysis using THF as eluent against polystyrene standards.
[b] Calculated according to the *DP* values of PNIPAM chain determined by ^{1}H NMR on the basis of M_n of OPV_5 obtained by MALDI-TOF.

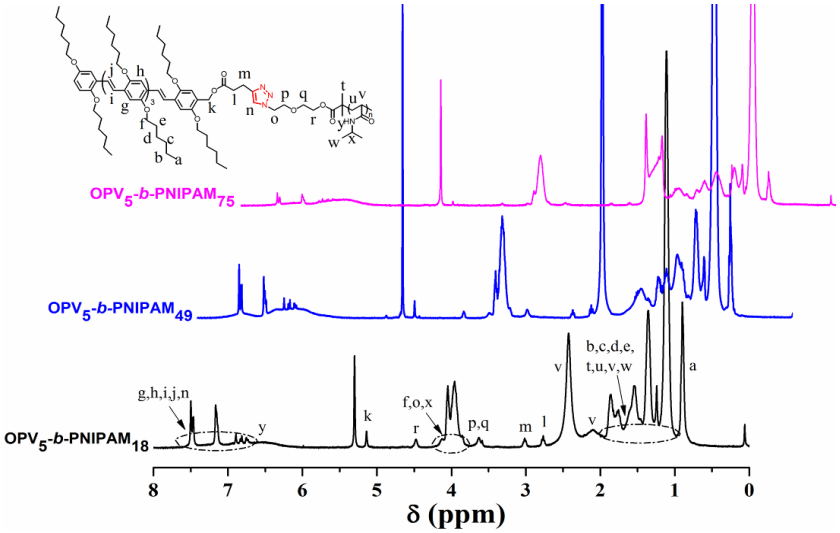

Figure 1. ^{1}H NMR spectra of OPV_5-*b*-$PNIPAM_{18}$, OPV_5-*b*-$PNIPAM_{49}$ and OPV_5-*b*-$PNIPAM_{75}$ in CD_2Cl_2. Degree of polymerization of PNIPAM (DP_{PNIPAM}) in each BCP was calculated based on the integrals for peaks "f+o+x" (S_{f+o+x}) and "a" (S_a) from OPV_5 segment ($DP_{PNIPAM} = (S_{f+o+x} - 13S_a/15)/(S_a/30)$).

Self-assembly of OPV-*b*-PNIPAM

Recently, we published a communication reporting the preparation of monodisperse fiber-like micelles containing an OPV-core of controllable length and composition in ethanol.[54] By taking advantage of the crystalline property of the OPV segment, these uniform OPV-based fiber-like micelles could be prepared by both the temperature-induced self-seeding route and the seeded growth strategy of living CDSA. This was the first example of self-seeding of an OPV-based BCP. The experiments involved a single sample of an OPV-based BCP (OPV_5-*b*-$PNIPAM_{49}$) under a single set of experimental conditions (solvent: ethanol; concentration: 0.05 mg/mL; temperature: 35-60ºC). In order to explore the scope and generality

of self-seeding of OPV-based copolymers, we synthesized a series of OPV-containing BCPs with the same OPV segment but PNIPAM chains with different chain lengths. We then carried out self-seeding experiments under different conditions in order to get more information and a deeper understanding of self-assembly, especially by self-seeding of OPV-containing BCPs.

We first investigated the self-assembly of OPV-*b*-PNIPAM in methanol, ethanol and isopropanol, selective solvents for PNIPAM. Samples of OPV-*b*-PNIPAM copolymers were suspended in these alcoholic solvents with a concentration of 0.1 mg/mL. Then, the mixtures were heated at 80ºC (65ºC for methanol) for 30 min to form clear solutions, followed by aging at room temperature (23ºC) for 48 h. For OPV_5-*b*-$PNIPAM_{18}$, long fiber-like micelles with lengths up to tens of micrometers and uniform width (14 nm) were formed in both ethanol and isopropanol, as seen in TEM images presented in Figures S4 and S5. In TEM images of samples prepared in methanol, one can see not only long fiber-like micelles with lengths L of several micrometers and short micelles with L ~ 100-300 nm, but also some complex two-dimensional platelet-like structures with fibers protruding from the ends (Figures 2A and 2B). For OPV_5-*b*-$PNIPAM_{49}$, fiber-like micelles with lengths of about several micrometers and uniform width (22 nm) were formed in all of these solvents (Figures 2C, S4 and S5). For OPV_5-*b*-$PNIPAM_{75}$, we observed both very short fiber-like micelles with L < 300 nm and few relatively long fiber-like micelles with L ~ 1 μm (Figures 2D and S4). These micelles have a uniform width of about 24 nm (Figure S5). Representative AFM images also demonstrate that fiber-like micelles were formed in ethanol for all of OPV-*b*-PNIPAM BCPs (Figure S6). All of these observations indicate that both solvent and the chain length of corona block affect the

Commented [F2]: delete

self-assembly of the OPV-*b*-PNIPAM BCPs. We present our ideas about how and why both the solvent and the chain length affect the self-assembly of OPV-*b*-PNIPAM BCPs in Supporting Information.

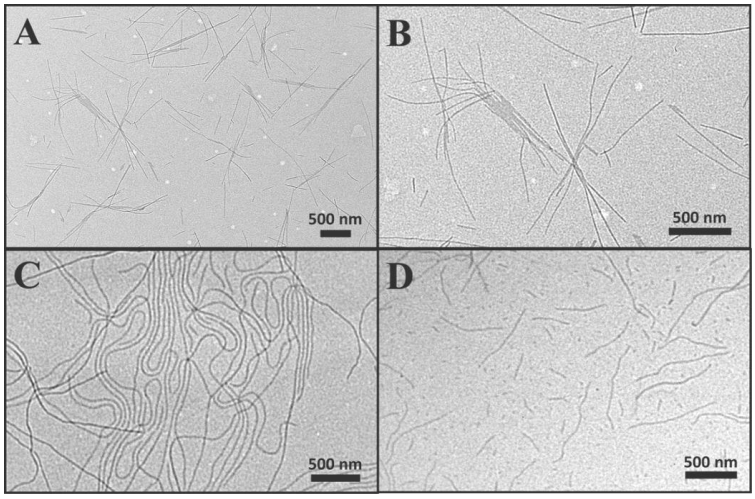

Figure 2. TEM images of fiber-like micelles obtained by heating the methanol solution (0.1 mg/mL) of (A and B) OPV_5-*b*-$PNIPAM_{18}$, (C) OPV_5-*b*-$PNIPAM_{49}$ and (D) OPV_5-*b*-$PNIPAM_{75}$ at 65°C for 30 min, followed by cooling at 23°C for 48 h. (B: higher magnification image from part of A).

Sonication to Obtain Micelle Fragment Seeds

To perform self-seeding experiments, we employed mild sonication (BRANSON model 1510 70 W ultrasonic cleaning bath) to fragment long micelles of each polymer in ethanol (0.1 mg/mL) prepared by the heating and cooling process described above. For OPV_5-*b*-$PNIPAM_{75}$, after sonication at 0°C for 2 min, we found a large number of short micelles with lengths below 50 nm and some surviving micelles with lengths of several hundred nanometers (Figure 3A and Table 2). However, after sonication for 5 min, only short micelles with lengths of 38±8 nm

(L_w/L_n = 1.04) were obtained (Figure 3B and Table 2). For OPV_5-*b*-$PNIPAM_{49}$, after sonication for 15 min at 0°C, the fragmented micelles had lengths of 219±125 nm (L_w/L_n = 1.32) (Figure 3C and Table 2). These lengths decreased to 40±10 nm (L_w/L_n = 1.06) after sonication for an additional 15 min (Figure 3D and Table 2).

Table 2. Characteristics of Fragmented Fiber-like Micelles of OPV-*b*-PNIPAM[a]

Sample	Sonication time (min)	Length (nm)[b]	L_w/L_n[b]
OPV_5-*b*-$PNIPAM_{75}$	2	187±198	2.12
	5	38±8	1.04
OPV_5-*b*-$PNIPAM_{49}$	15	219±125	1.32
	30	40±10	1.06
OPV_5-*b*-$PNIPAM_{18}$	30	135±48	1.23
	60	96±46	1.22
	120	81±28	1.12
	180	41±13	1.10

[a]: The fragmented fiber-like micelles were obtained by sonication of pristine fiber-like micelles, which were prepared by heating OPV-*b*-PNIPAM BCPs (0.1 mg/mL) at 80°C for 30 min, followed by cooling at 23°C for 48 h, at 0°C for different time. The lengths of fiber-like micelles were measured from their TEM images and the values were obtained by over 200 readings.

[b] L_n , L_w and σ are the number-average micelle length, weight-average micelle length, and the standard deviation of micelle length distribution, respectively, as calculated from the histograms of the length distributions.

For OPV_5-*b*-$PNIPAM_{18}$, sonication was less effective. The length of the fragmented micelles after sonication for 30 min was still 135±48 nm (L_w/L_n = 1.23) with a broad length distribution (Figure 3E and Table 2). We then further extended the sonication time to 1 h, 2 h and 3 h for OPV_5-*b*-$PNIPAM_{18}$ and characterized the length of fragmented micelles by TEM. The length of fragmented decreased to 96±46 nm (L_w/L_n = 1.22), 81±28 nm (L_w/L_n = 1.12) and 41±13 nm

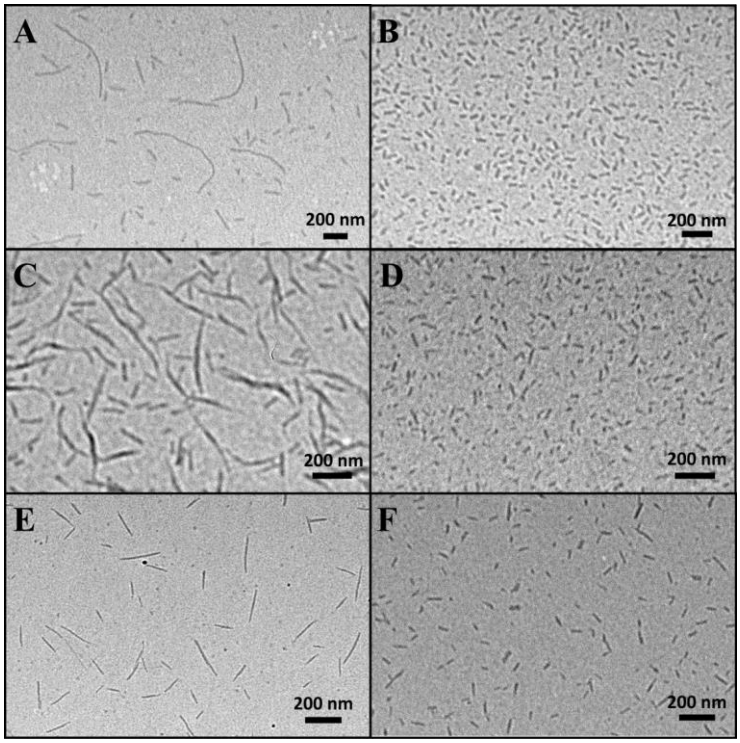

Figure 3. TEM images of fragmented micelles of OPV_5-*b*-$PNIPAM_{75}$ obtained by sonication for 2 (A) and 5 (B) min, OPV_5-*b*-$PNIPAM_{49}$ after sonication for 15 (C) and 30 (D) min and OPV_5-*b*-$PNIPAM_{18}$ after sonication for 30 min (E) and 3 h (F) at 0°C. Long micelles of OPV_5-*b*-$PNIPAM_{18}$, OPV_5-*b*-$PNIPAM_{49}$ and OPV_5-*b*-$PNIPAM_{75}$ in ethanol (0.1 mg/mL) for fragmentation by sonication were prepared by heating the block copolymer (0.1 mg/mL) at 80°C for 30 min, followed by cooling at 23°C for 48 h.

(L_w/L_n = 1.10) for sonication times of 1 h, 2 h and 3 h, respectively (Figures 3F and S7, Table 2). GPC analysis shows that there was no detectable degradation of OPV_5-*b*-$PNIPAM_{18}$ over the 3 h sonication (Figure S8). These results demonstrate that fiber-like micelles of OPV-*b*-PNIPAM became easier to fragment with the increase in PNIPAM chain length.

In order to examine the influence of PNIPAM chain length on the packing of OPV segments within the core, we performed GIWAXS measurements on thin-film samples of fiber-like

micelles of OPV-*b*-PNIPAM. The d-spacing values of the OPV segments, which are attributed to π-π stacking of OPV segments, are 3.87 Å (q =16.2 nm^{-1}) for OPV_5-*b*-$PNIPAM_{18}$, 3.93 Å (q =16.0 nm^{-1}) for OPV_5-*b*-$PNIPAM_{49}$ and 4.04 Å (q =15.5 nm^{-1}) for OPV_5-*b*-$PNIPAM_{75}$ (Figure S9). These results suggest that the OPV segments within the micelle core stack much tighter for OPV-*b*-PNIPAM BCPs with a shorter PNIPAM chain due to the decrease in steric repulsion within the PNIPAM layer. In addition, the increase in PNIPAM chain length should increase the solubility of OPV-*b*-PNIPAM in the various solvents. Accordingly, the resistance of the micelles to fragmentation is enhanced with the decrease in PNIPAM chain length.

Heating Time Effect on Self-seeding

We then tested the influence of heating time on the self-seeding behavior of OPV-*b*-PNIPAM in ethanol. Aliquots of seed micelles (0.05 mg/mL in ethanol) of OPV_5-*b*-$PNIPAM_{49}$ (L_n = 44 nm, L_w/L_n = 1.27, Figure S10) were heated at 50°C for various times (15, 30, 60, 90 and 120 min), allowed to cool in air, and then aged for 48 h (Scheme 1). Fiber-like micelles with an average length (L_n) of 210 nm, a length distribution (L_w/L_n) of 1.06 and a uniform width (22 nm) were formed for the sample heated for 15 min (Figures 4A and 4D, Table S1). As the heating time was extended to 30 min, L_n increased to 292 nm (Figures 4B and 4D). The values of L_n did not vary significantly with longer heating times (60, 90 and 120 min) within the experimental error, and all of the micelles formed at different heating times had narrow length distributions (L_w/L_n < 1.10) and uniform widths (*ca*. 22 nm, Figures 4C, 4D and S10). We also examined the influence of heating time on L_n for micelles for OPV_5-*b*-$PNIPAM_{18}$

(Figure S11 and Table S2). Here we found L_n = 204 nm (L_w/L_n = 1.16) after heating for 15 min, increased to 305 nm (L_w/L_n = 1.10) after heating for 30 min. Further annealing (60, 90 and 120 min) did not lead to any obvious change in L_n.

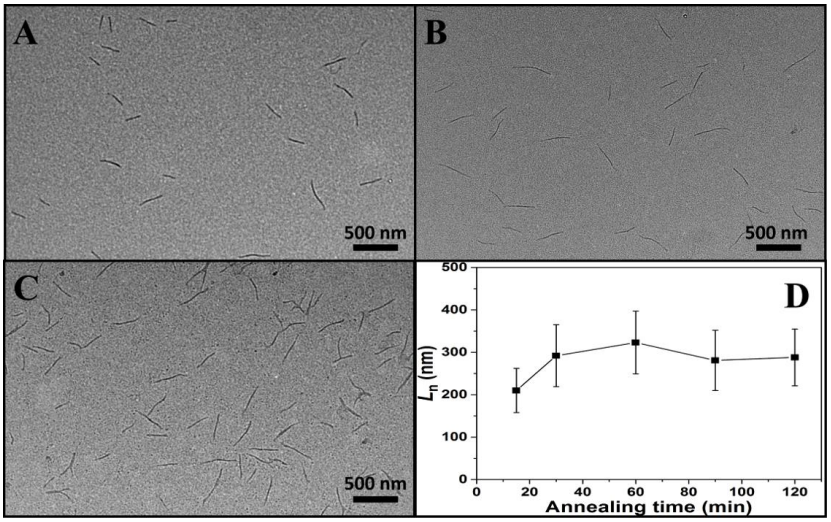

Figure 4. TEM images of fiber-like micelles of OPV_5-*b*-$PNIPAM_{49}$ obtained by annealing the seeds in ethanol (0.05 mg/mL in ethanol) for 15 (A), 30 (B) and 120 (C) min at 50°C, followed by aging at 23°C for 48 h. (D) L_n values of micelles of OPV_5-*b*-$PNIPAM_{49}$ versus annealing time at 50°C (error bars represent the standard deviation σ of the length distributions). The seed micelles of OPV_5-*b*-$PNIPAM_{49}$ were obtained by sonication of the long fiber-like micelles of OPV_5-*b*-$PNIPAM_{49}$ (0.1 mg/mL in ethanol) at 0°C for 30 min. The seed micelle solution was diluted to 0.05 mg/mL for the annealing.

The results described in the previous paragraph are consistent with those reported by Qian *et al*., who examined the influence of heating time on the self-seeding of PI_{637}-*b*-PFS_{53} in decane. They found that L_n of micelles obtained by heating for 10 min at 64°C (L_n = 879 nm) was a bit shorter than those of micelles prepared by heating for 2h (L_n = 927 nm) and 24 h (L_n = 924 nm).[8] Similar results were reported for the self-seeding of poly(2-(perfluorooctyl)ethyl methacrylate-*b*-poly(2-vinyl pyridine) ($PFMA_{41}$-*b*-$P2VP_{68}$), which formed fiber-like micelles

with a liquid crystalline PFMA core in isopropanol.[53] Here L_n increased from 193 nm to 309 nm as the heating time was increased from 5 min to 30 min at 65ºC, but remained constant for longer heating times.[53] Results from others and our current system demonstrate that the dissolution of seed micelles at a given temperature occurs under thermodynamic control.[9,59-61]

Solvent Effect on Self-seeding

The influence of solvent on the self-seeding of OPV-*b*-PNIPAM was examined by performing the self-seeding experiments in different alcoholic solvents (methanol, ethanol and isopropanol). The pristine long fiber-like micelles of OPV_5-*b*-$PNIPAM_{49}$ in each solvent were prepared by the heating and cooling process described above. TEM images of the micelles obtained are shown in Figures 2C (methanol), S4C (ethanol) and S4D (isopropanol). Seed micelles for self-seeding experiments were obtained by the sonication of solutions of each long micelle sample at 0ºC for 30 min. L_n values of the fragmented micelles of OPV_5-*b*-$PNIPAM_{49}$ were 31 nm (L_w/L_n = 1.18) in methanol, 44 nm (L_w/L_n = 1.27) in ethanol and 52 nm (L_w/L_n = 1.14) in isopropanol. These solutions of micelle fragment (0.05 mg/mL) were then heated at different temperatures (35ºC to 60ºC), followed by cooling in air and aging for 48 h. In methanol, the length distribution was rather broad. Some long micelles with lengths of several hundred nanometers were formed after the seed micelle solution was heated at 47ºC and 53ºC, as shown in Figures 5A and 5B. One can also see many short micelles with lengths below 100 nm. These results are summarized in Table S3.

In contrast, OPV_5-*b*-$PNIPAM_{49}$ formed uniform fiber-like micelles in ethanol and

isopropanol after heating at 53ºC, as shown in the TEM images in Figures 5C and 5D. Additional TEM images and histograms of the length distributions are presented in Figures S12 and S13 and length information is summarized in Tables S4 and S5.

In Figure 5E, we plotted L_n values of the micelles obtained in ethanol and isopropanol versus annealing temperature. Values of L_n for micelles in ethanol increased gradually from 74 nm to 172 nm as the temperature was increased from 35ºC to 47ºC and then increased abruptly to 1152 nm as the temperature was increased to 60ºC (Figure S12 and Table S4). The fiber-like micelles obtained in isopropanol also increased in length slowly from 62 nm to 203 nm when the temperature was increased from 35ºC to 47ºC, and then the length increased sharply to 1127 nm as the temperature was elevated to 57ºC (Figure S13 and Table S5). All of the fiber-like micelles obtained in both ethanol and isopropanol have narrow length distributions ($L_w/L_n \leq 1.14$) as indicated by distributions indicated in Figure 5E. One can see that there is a dramatic increase in the length of micelles obtained after heating the OPV_5-*b*-$PNIPAM_{49}$ micelle fragment solutions at temperatures above 47ºC in ethanol and isopropanol.

Considering the constant mass of copolymer in each solution and constant mass per unit length of micelle as demonstrated by the same width of the micelles before and after the heating and cooling process, we are able to calculate the fraction of surviving micelle fragments at each temperature (P_s). This calculation (Equation 1 and Scheme 1) takes into account the initial length of seed micelles (L_0) and the final length of micelles (L_t), and assumes that there is only a negligible amount of soluble copolymer at room temperature.

$$P_s = L_0/L_t \quad (1)$$

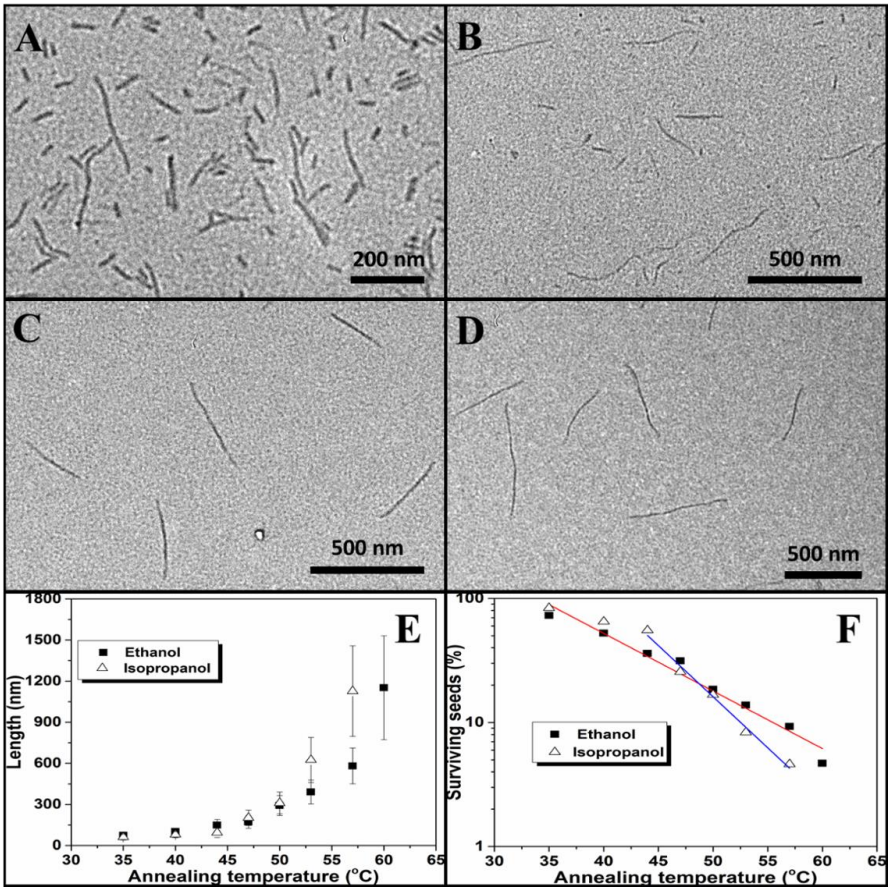

Figure 5. TEM images of fiber-like micelles of OPV_5-*b*-$PNIPAM_{49}$ obtained by annealing the corresponding seeds in methanol (0.05 mg/mL) at 47°C (A) and 53°C (B) and in ethanol (C) (0.05 mg/mL) and isopropanol (D) (0.05 mg/mL) at 53°C. (E) L_n values of micelles of OPV_5-*b*-$PNIPAM_{49}$ obtained in ethanol and isopropanol versus annealing temperature (error bars represent the standard deviation σ of the length distribution). (F) Semilogarithmic plots of the fraction of surviving seeds in ethanol and isopropanol versus annealing temperature.

For example, using the data shown in Figure 5E, we calculated the fraction of surviving seeds at every temperature and plotted these values against the annealing temperature for each sample (Figure 5F). The fraction of surviving seeds decreased exponentially with the increasing

temperature for the samples in both ethanol and isopropanol. This is a key characteristic of self-seeding.[7-9] It is interesting to note that the dissolution of seed micelles in isopropanol is more sensitive to annealing temperature, ranging from 45°C to 57°C, than that in ethanol, as indicated by a fitting line with a higher slope in Figure 5F. For example, only 4.6% of seeds survived upon heating at 57°C for 30 min in isopropanol, whereas 7.6% of seeds survived in ethanol under the same conditions.

These observations indicate that the polarity of the solvents affected the self-seeding of OPV-*b*-PNIPAM. The solubility parameter of OPV can be estimated to be about 18.7 $MPa^{1/2}$, based upon the value for poly[2-methoxy-5(20-ethylhexyloxy)-1,4- phenylenevinylene] (MEH-PPV). The corresponding value of PNIPAM is 23.5 $MPa^{1/2}$, closer to the solubility parameter of isopropanol (23.6 $MPa^{1/2}$) than ethanol (26.5 $MPa^{1/2}$) or methanol (29.6 $MPa^{1/2}$) (Table 3).[62-64] Thus, methanol is the poorest solvent for OPV on the basis of difference between the solubility parameters of OPV and those of the solvents (Table 3) and also a somewhat poorer solvent for PNIPAM. The solvophobic effect of OPV-*b*-PNIPAM in methanol should be more pronounced than those in ethanol and isopropanol, which might lead to a faster aggregation of OPV-*b*-PNIPAM in methanol upon cooling. We speculate that this relative fast aggregation might favor the self-nucleation of the OPV block, and thus, promote the formation of short fiber-like micelles. Previous work on self-seeding of PFS_{53}-*b*-PI_{637} and PFS_{60}-*b*-$PDMS_{660}$ in decane showed that the seed micelles of PFS_{60}-*b*-$PDMS_{660}$ were harder to dissolve than those of PFS_{53}-*b*-PI_{637}, where decane is a better solvent for PDMS than for PI.[8] Here, the seed micelles of OPV_5-*b*-$PNIPAM_{49}$ seem to be harder to dissolve in isopropanol than in ethanol in the

temperature range from 45ºC to 57ºC. This observation might show that the solubility effect for self-seeding of OPV-*b*-PNIPAM is different from that for PFS-based copolymers.

Table 3. Solubility Parameters (δ) of Polymers and Solvents

Sample	OPV[a]	PNIPAM[b]	PDEAEMA[b]	Methanol	Ethanol	Isopropanol
δ ($MPa^{1/2}$)	18.7	23.5	18.3	29.6	26.5	23.6

[a]: The solubility parameter of poly[2-methoxy-5(20-ethylhexyloxy)-1,4-phenylenevinylene] (MEH-PPV) is used here for OPV segment. [62]
[b]: The solubility parameters of PNIPAM[63] and PDEAEMA[64] segments were taken from the literature.

Polymer Concentration Effect on Self-seeding

To investigate the influence of OPV-*b*-PNIPAM BCP concentration on self-seeding, we chose to examine the self-seeding of OPV_5-*b*-$PNIPAM_{49}$ in a single solvent, ethanol. A seed micelle sample of OPV_5-*b*-$PNIPAM_{49}$ (Figure 6A, 0.1 mg/mL in ethanol, L_n = 44 nm, L_w/L_n = 1.27) was diluted with ethanol to afford seed solutions with concentrations of 0.05 and 0.02 mg/mL, respectively. Aliquots of those seed micellar solutions were heated at various temperatures (from 35ºC to 60ºC) for 30 min, followed by cooling and aging at room temperature for 48 h. Monodisperse fiber-like micelles with similar uniform widths (22 nm) were obtained, and the L_n values of the micelles increased with the increasing temperature for the samples with different concentrations (Figures 6B-6E). (Additional TEM images of micelles obtained under different conditions, along with values of L_n, L_w/L_n and σ/L_n of all of these samples, as well as histograms of the length distribution of these micelles are shown in Figures

S12, S14 and S15, Tables S4, S6 and S7). The fraction of surviving fragments decreased exponentially with increasing heating temperature in the range from 35ºC to 60ºC (57ºC for the sample with a concentration of 0.02 mg/mL). As mentioned above, this phenomenon is a key characteristic of self-seeding. These results indicated that the uniform fiber-like micelles with various lengths can be obtained by self-seeding with different polymer concentrations.

The data in Figures 6E and 6F also show that the L_n values of the micelles obtained by self-seeding is dependent on the concentration of the seed micelle solution. Higher concentrations led to the formation of shorter micelles at the same annealing temperature (Figure 6E). For example, for samples annealed at 53ºC, we found L_n = 633 nm at 0.02 mg/mL, 391 nm at 0.05 mg/mL, and 334 nm at 0.10 mg/mL. It thus appears that more seed micelles survive for the samples with a higher concentration at the same temperature (Figure 6F). We calculate that about 87% of the seed micelles at 0.10 mg/mL dissolved at 53°C, 89% at 0.05 mg/mL and 93% at 0.02 mg/mL (Figure 6F). This phenomenon implies that the seed micelles with a lower concentration are easier to dissolve than those with a higher concentration.

At this time, we do not have a clear explanation for the polymer concentration effect on the self-seeding. However, this effect is not unique for the self-seeding of OPV_5-*b*-$PNIPAM_{49}$. Li *et al.* also found that the polymer concentration affected the mean length of fiber-like micelles of PFMA-*b*-P2VP obtained by self-seeding.[53] They found that L_n of fiber-like micelles obtained by annealing of seed micelles at 65ºC in isopropanol decreased from 325 nm to 214 nm when the concentration of seed micelle increased from 0.05 mg/mL to 1.0 mg/mL. If we assume that there is a dynamic equilibrium between the dissolution of seed micelles to form free polymers and

re-crystallization of these dissolved free polymers onto the surviving seed micelles, the increase in the initial concentration of seed micelles may lead to less dissolution of the seed micelles. A larger number of surviving seed micelles would lead to lower values of L_n upon micelle regrowth after cooling to room temperatures.

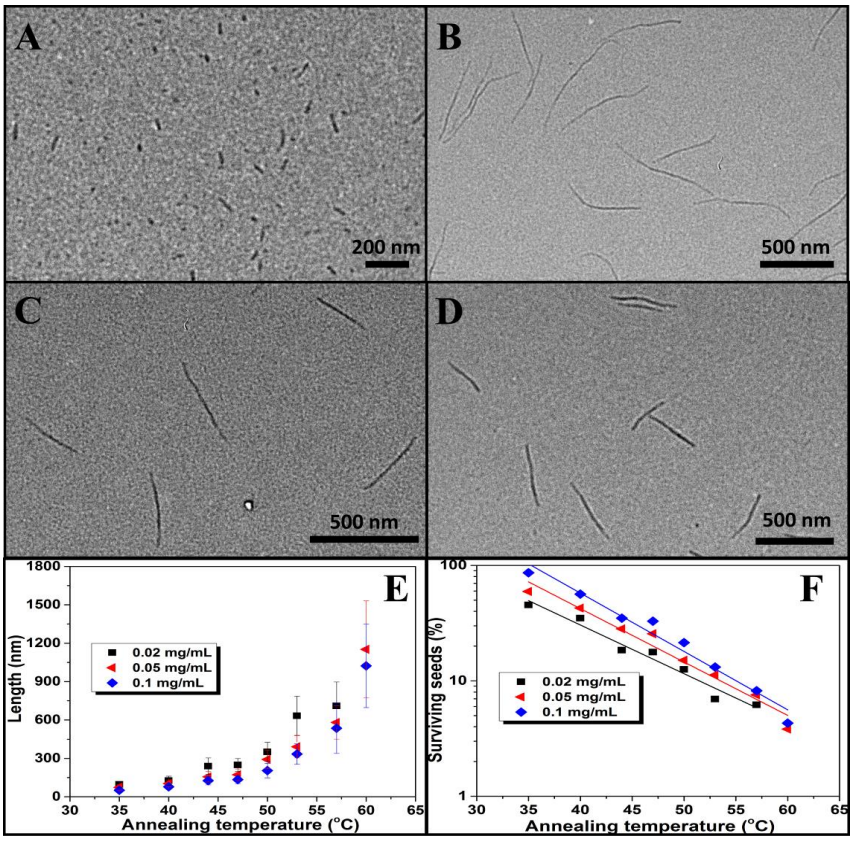

Figure 6. TEM images of seeds (A) and fiber-like micelles of OPV_5-*b*-$PNIPAM_{49}$ obtained by annealing the seeds in ethanol with a concentration of 0.02 (B), 0.05 (C) and 0.1 (D) mg/mL at 53°C. (E) L_n values of micelles of OPV_5-*b*-$PNIPAM_{49}$ obtained with different concentrations versus annealing temperature (error bars represent the standard deviation σ of length distribution). (F) Semilogarithmic plot of the fraction of surviving seeds with different concentrations versus annealing temperature.

PNIPAM Chain Length Effect on Self-seeding

To test the effect of the chain length of PNIPAM segment on self-seeding, we chose to examine all three polymers in a single solvent, ethanol, at the same concentration (0.1 mg/mL). The seed micelle fragments that we used were characterized by L_n = 40 nm (L_w/L_n = 1.04) for OPV_5-*b*-$PNIPAM_{18}$, L_n = 44 nm (L_w/L_n = 1.27) for OPV_5-*b*-$PNIPAM_{49}$ and L_n = 38 nm (L_w/L_n = 1.13) for OPV_5-*b*-$PNIPAM_{75}$. For OPV_5-*b*-$PNIPAM_{18}$ and OPV_5-*b*-$PNIPAM_{49}$, fiber-like micelles with narrow length distributions ($L_w/L_n \leq 1.14$) were obtained at annealing temperatures ranging from 35ºC to 60ºC (Figures 7A, 7B, S14 and S16, and Tables S6 and S8). For OPV_5-*b*-$PNIPAM_{75}$, fiber-like micelles ($L_w/L_n \leq 1.11$) with lengths ranging from 50 nm to 665 nm were obtained by self-seeding (Figures 7C and S17, and Table S9). This observation demonstrates the generality of self-seeding for OPV-*b*-PNIPAM.

One can see that the lengths of micelles increase with annealing temperature and exhibit a sharper increase as the temperature is raised above 47ºC for all of samples (Figure 7E). In addition, the fraction of surviving fragments decreased exponentially with increasing heating temperature (Figure 7F). It is interesting to notice that the values of the slopes of fitting lines for each sample were almost same. This result might indicate that the dissolution of seed micelles is independent of the chain length of PNIPAM in the temperature range from 35ºC to 57ºC. However, we found that fiber-like micelles with a broad length distribution formed at 60ºC for OPV_5-*b*-$PNIPAM_{75}$ (Figure 9D), whereas uniform micelles still can be obtained for OPV_5-*b*-$PNIPAM_{18}$ and OPV_5-*b*-$PNIPAM_{49}$ under the same conditions (Figures 7A and 7B). We attribute the broad distribution to the complete dissolution of the polymer at this temperature.

Subsequently micelles form by self-nucleation upon cooling. Thus, this observation suggests that the seed micelles of OPV_5-*b*-$PNIPAM_{75}$ can be completely dissolved at a lower temperature than those of OPV_5-*b*-$PNIPAM_{18}$ and OPV_5-*b*-$PNIPAM_{49}$.

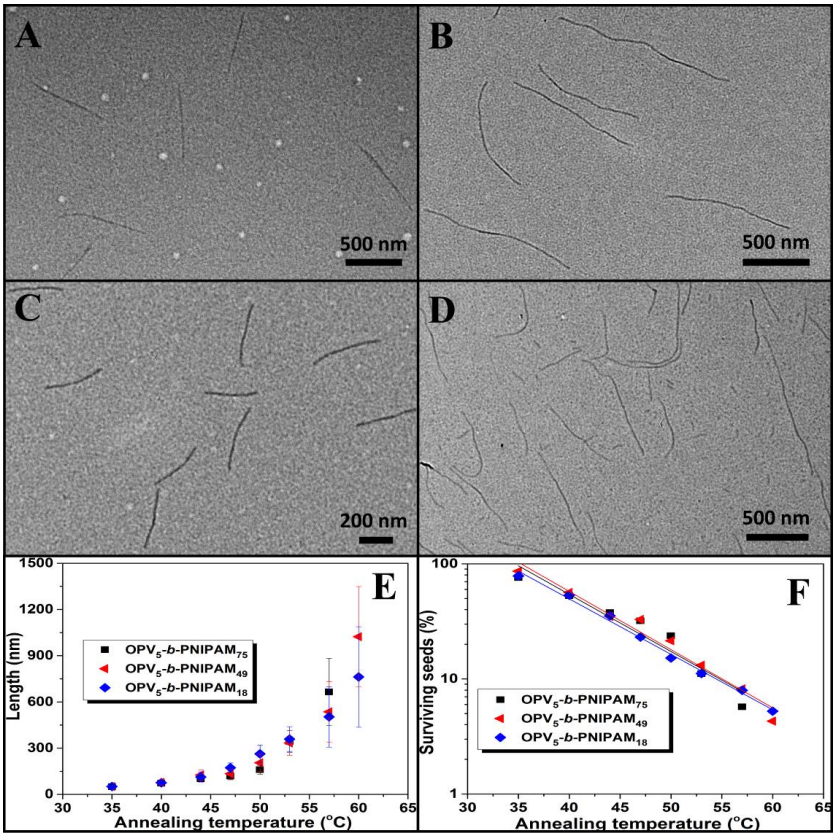

Figure 7. TEM images of fiber-like micelles of OPV_5-*b*-$PNIPAM_{18}$ (A) and OPV_5-*b*-$PNIPAM_{49}$ (B) obtained by annealing the corresponding seeds in ethanol (0.1 mg/mL) at 60°C, and OPV_5-*b*-$PNIPAM_{75}$ obtained by annealing the seeds in ethanol (0.1 mg/mL) at 53°C (C) and 60°C (D). (E) L_n values of micelles of OPV_5-*b*-$PNIPAM_{18}$, OPV_5-*b*-$PNIPAM_{49}$ and OPV_5-*b*-$PNIPAM_{75}$ versus annealing temperature (error bars represent the standard deviation σ of the length distribution). (F) semilogarithmic plot of the fraction of surviving seeds of OPV_5-*b*-$PNIPAM_{18}$, OPV_5-*b*-$PNIPAM_{49}$ and OPV_5-*b*-$PNIPAM_{75}$ in solution versus annealing temperature.

Extension of Self-seeding to OPV-*b*-poly(2-(diethylamino)ethyl methacrylate)

To examine if self-seeding can be applied to other OPV-containing BCPs, we also synthesized a diblock copolymer containing OPV_5 and poly(2-(diethylamino)ethyl methacrylate) (PDEAEMA) segments (Scheme S3), OPV_5-*b*-$PDEAEMA_{60}$. We used a similar synthetic route as that used for the preparation of OPV-*b*-PNIPAM (Figures S18 and S19, see SI for preparation and characterization).

Fiber-like micelles with uniform width were obtained by heating an ethanol solution of OPV_5-*b*-$PDEAEMA_{60}$ (0.05 mg/mL) for 30 min, followed by cooling in air and aging at room temperature for 48 h (Scheme 1 and Figure S20). Subsequently, seed micelle fragments (L_n = 41 nm, L_w/L_n = 1.10, Figure 8A, see SI for details) were obtained by sonication at 0°C for 3 h. Using a similar self-seeding protocol, uniform fiber-like micelles ($L_w/L_n \leq 1.06$) with uniform width, but different lengths in the range from 48 nm to 444 nm were obtained (Figures 8B-8E and details of characterization of micelles obtained at different temperatures are shown in Figure S21 and Table S10). The surviving seed percentage also decreased exponentially with the increasing temperature (Figure 8F). These results indicate that self-seeding is also applicable for other OPV-containing BCPs to vary the length of the fiber-like micelles (Scheme 1).

Another important message we get from this result is the effect of the corona-forming chain on the resistance of the micelles to fragmentation upon sonication and its effect on self-seeding of the OPV-based copolymers. For micelles of OPV_5-*b*-$PDEAEMA_{60}$, although the mean number of repeat units of PDEAEMA is 60, longer than that of PNIPAM in OPV_5-*b*-$PNIPAM_{49}$, this sample required a much longer time of sonication (3 h) to obtain seed micelles of

OPV_5-*b*-$PDEAEMA_{60}$ with $L_n \approx 40$ nm. This means that the micelles of OPV_5-*b*-$PDEAEMA_{60}$ had a higher resistance to fragmentation by sonication than those of OPV_5-*b*-$PNIPAM_{49}$. In addition, we note that the fraction of surviving seed micelles of OPV_5-*b*-$PDEAEMA_{60}$ is higher than that of OPV_5-*b*-$PNIPAM_{49}$ at the same annealing temperature (Figure 8F). This result indicates that the seed micelles of OPV_5-*b*-$PDEAEMA_{60}$ were harder to dissolve than those of OPV_5-*b*-$PNIPAM_{49}$.

These results are somewhat surprising. They are in apparent contrast with the observations (Table 2) that corona repulsion should promote fragmentation of the core-crystalline micelles upon sonication and the dissolution of micelle fragments upon heating, and we initially anticipated more corona repulsion in micelles with the longer $PDEAEMA_{60}$ corona-forming chains that for micelles with $PNIPAM_{49}$. The difference in behavior may be related to the difference in solvent quality of ethanol for PDEAEMA and PNIPAM, as reflected in their solubility parameters (PDEAEMA, $\delta = 18.3$ $MPa^{1/2}$; PNIPAM, $\delta = 23.5$ $MPa^{1/2}$; ethanol, $\delta = 26.5$ $MPa^{1/2}$).[62-64] A higher solubility of OPV_5- $PNIPAM_{49}$ might lead to increased swelling of the corona chains, which in turn imparted weaker resistance toward sonication and dissolution upon heating.

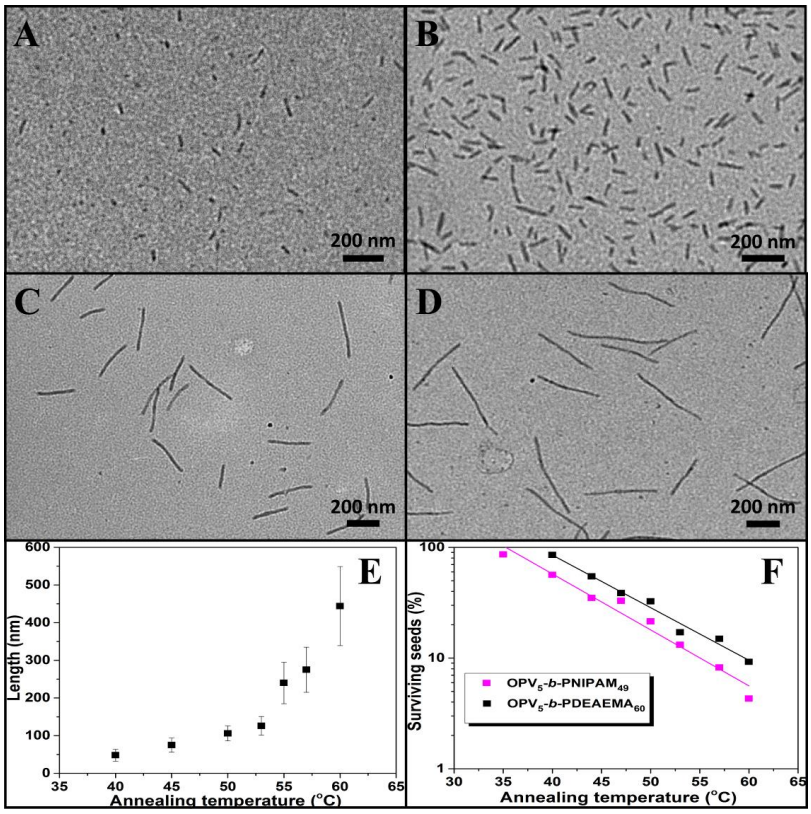

Figure 8. TEM images of (A) seeds, fiber-like micelles of OPV_5-*b*-$PDEAEMA_{60}$ obtained by annealing the seeds in ethanol (0.05 mg/mL) at (B) 45°C, (C) 55°C, and (D) 60°C. TEM samples were stained with phosphotungstic acid. (E) L_n values versus annealing temperature (error bars represent the standard deviation σ of the length distribution). (F) semilogarithmic plots of the fraction of surviving seeds of OPV_5-*b*-$PNIPAM_{49}$ and OPV_5-*b*-$PDEAEMA_{60}$ in solution (ethanol, 0.05 mg/mL) versus annealing temperature.

Summary

In summary, a series of diblock copolymers containing the same OPV segment, but different corona-forming blocks (OPV_5-*b*-$PNIPAM_{18}$, OPV_5-*b*-$PNIPAM_{49}$, OPV_5-*b*-$PNIPAM_{75}$ and OPV_5-*b*-$PDEAEMA_{60}$) were synthesized, and their self-assembly in alcohol solvents (methanol,

ethanol and isopropanol) was investigated. We found that both solvent and the chain length of the PNIPAM block affected the self-assembly behavior. OPV_5-*b*-$PNIPAM_{18}$ in methanol exhibited the most complex behavior. It not only formed fiber-like micelles of uniform width, it also formed some platelet-like structures with fibers protruding from the ends. In contrast, OPV_5-*b*-$PNIPAM_{18}$ self-assembled into fiber-like micelles with lengths of several micrometers in both ethanol and isopropanol. For OPV_5-*b*-$PNIPAM_{49}$, long fiber-like micelles with lengths of several micrometers were formed in these solvents, but only short fiber-like micelles with length below 1 μm were formed upon self-nucleated self-assembly by OPV_5-*b*-$PNIPAM_{75}$.

Studies of the sonication conditions needed to prepare appropriately short (*ca*. 50 nm) seed micelles indicate that the length of PNIPAM block affects the resistance of micelles toward fragmentation. The longer the PNIPAM chain is, the easier was the fragmentation of the fiber-like micelles. We attribute this effect to stronger repulsion in the solvent-swollen corona chains. An investigation of the influence of heating time on the self-seeding process shows that the dissolution of seed micelle fragments of OPV-*b*-PNIPAM operated under thermodynamic control. The polarity of solvent also plays a role. A relatively poor solvent for the BCP would result in more rapid self-nucleation and thus a broader length distribution. For example, fiber-like micelles of OPV_5-*b*-$PNIPAM_{49}$ with a broad length distribution were obtained by self-seeding in methanol, likely due to the self-nucleation. Although the self-seeding technique can be carried out in various solvents, with different copolymer concentrations and for OPV-containing copolymers consisting of different corona-forming blocks, certain conditions favor the formation of fiber-like micelles of controlled lengths and narrow length distribution.

These factors include a better solvent for the BCP, a more soluble corona-forming segment, and a lower concentration of copolymer. They also tend to result in a lower dissolution temperature for the coil-crystalline micelle fragments upon heating.

Overall, this study demonstrates that self-seeding of CDSA is a versatile and convenient tool to prepare uniform fiber-like micelles of controlled length with an OPV core, but different corona-formation blocks. Given the wide application of OPV-based BCPs in electronics and attractive properties of π-conjugated fiber, the self-seeding of OPV-based BCPs exhibits great potential in the fabrication of OPV-fiber-based functional nanomaterials.

ASSOCIATED CONTENT

Supporting Information

Experimental procedures on the synthesis and characterization of polymers and micelles: GPC curves and ^{1}H NMR spectra of azide-terminated PNIPAM, azide-terminated PDEAEMA, OPV-*b*-PNIPAM and OPV-*b*-PDEAEMA; TEM images of original micelles of OPV_5-*b*-$PNIPAM_{18}$, OPV_5-*b*-$PNIPAM_{49}$, OPV_5-*b*-$PNIPAM_{75}$ and OPV_5-*b*-$PDEAEMA_{60}$ prepared by directly heating and cooling; AFM height images of OPV_5-*b*-$PNIPAM_{18}$, OPV_5-*b*-$PNIPAM_{49}$ and OPV_5-*b*-$PNIPAM_{75}$; GIWAXS spectra of dried OPV_5 and fiber-like micelles of OPV_5-*b*-$PNIPAM_{18}$, OPV_5-*b*-$PNIPAM_{49}$ and OPV_5-*b*-$PNIPAM_{75}$ in ethanol; TEM images, histograms and length information of fiber-like micelles of OPV_5-*b*-$PNIPAM_{18}$, OPV_5-*b*-$PNIPAM_{49}$, OPV_5-*b*-$PNIPAM_{75}$ and OPV_5-*b*-$PDEAEMA_{60}$ obtained under different conditions; additional comments on the formation of fiber-like micelles and two-dimensional

platelet-like structures by OPV-*b*-PNIPAM. The Supporting Information is available free of charge on the ACS Publications website.

AUTHOR INFORMATION

Corresponding Author

cfeng@mail.sioc.ac.cn; mwinnik@chem.utoronto.ca; xyhuang@mail.sioc.ac.cn

ORCID

Chun Feng: 0000-0003-1034-9831

Mitchell A. Winnik: 0000-0002-2673-2141

Xiaoyu Huang: 0000-0002-9781-972X

Notes

The authors declare no competing financial interests.

ACKNOWLEDGMENTS

The authors thank the financial support from National Key Research & Development Program of China (2016YFA0202900), National Basic Research Program of China (2015CB931900), National Natural Science Foundation of China (51373196 and 21504102), Strategic Priority Research Program of the Chinese Academy of Sciences (XDB20000000), Youth Innovation Promotion Association of Chinese Academy of Sciences (2016233) and

Shanghai Scientific and Technological Innovation Project (16JC1402500 and 16520710300). MAW thanks NSERC Canada for its financial support.

REFERENCES

(1) Zhang, L. F.; Yu, K.; Eisenberg, A. Ion-Induced Morphological Changes in "Crew-Cut" Aggregates of Amphiphilic Block Copolymers. *Science* **1996**, *272*, 1777-1779.

(2) Zhang, L. F.; Eisenberg, A. Multiple Morphologies and Characteristics of "Crew-Cut" Micelle-like Aggregates of Polystyrene-*b*-poly(acrylic acid) Diblock Copolymers in Aqueous Solutions. *J. Am. Chem. Soc.* **1996**, *118*, 3168-3181.

(3) Mai, Y. Y.; Eisenberg, A. Self-assembly of Block Copolymers. *Chem. Soc. Rev.* **2012**, *41*, 5969-5985.

(4) Ge, Z. S.; Liu, S. Y. Functional Block Copolymer Assemblies Responsive to Tumor and Intracellular Microenvironments for Site-Specific Drug Delivery and Enhanced Imaging Performance. *Chem. Soc. Rev.* **2013**, *42*, 7289-7325.

(5) Cameron, N. S.; Corbierre, M. K.; Eisenberg, A., 1998 E.W.R. Steacie Award Lecture Asymmetric amphiphilic block copolymers in solution: a morphological wonderland. *Can. J. Chem.* **1999**, *77*, 1311-1326.

(6) Blanazs, A.; Armes, S. P.; Ryan, A. J. Self-Assembled Block Copolymer Aggregates: From Micelles to Vesicles and their Biological Applications. *Macromol. Rapid Commun.* **2009**, *30*, 267-277.

(7) Qian, J. S.; Guerin, G.; Lu, Y. J.; Cambridge, G.; Manners, I.; Winnik, M. A. Self- Seeding

in One Dimension: An Approach To Control the Length of Fiberlike Polyisoprene-Polyferrocenylsilane Block Copolymer Micelles. *Angew. Chem. Int. Ed.* **2011**, *50*, 1622-1625.

(8) Qian, J. S.; Lu, Y. J.; Chia, A.; Zhang, M.; Rupar, P. A.; Gunari, N.; Walker, G. C.; Cambridge, G.; He, F.; Guerin, G.; Manners, I.; Winnik, M. A. Self-Seeding in One Dimension: A Route to Uniform Fiber-like Nanostructures from Block Copolymers with a Crystallizable Core-Forming Block. *ACS Nano* **2013**, *7*, 3754-3766.

(9) Xu, J. J.; Ma, Y.; Hu, W. B.; Rehahn, M.; Reiter, G. Cloning Polymer Single Crystals through Self-Seeding. *Nat. Mater.* **2009**, *8*, 348-353.

(10) Wang, X. S.; Guerin, G.; Wang, H.; Wang, Y. S.; Manners, I.; Winnik, M. A. Cylindrical Block Copolymer Micelles and Co-Micelles of Controlled Length and Architecture. *Science* **2007**, *317*, 644-647.

(11) Qiu, H. B.; Hudson, Z. M.; Winnik, M. A.; Manners, I. Multidimensional Hierarchical Self-Assembly of Amphiphilic Cylindrical Block Co-Micelles. *Science* **2015**, *347*, 1329-1332.

(12) Boott, C. E.; Gwyther, J.; Harniman, R. L.; Hayward, D. W.; Manners, I. Scalable and Uniform 1D Nanoparticles by Synchronous Polymerization, Crystallization and Self-Assembly. *Nat. Chem.* **2017**, *9*, 785-792.

(13) Li, X. Y.; Gao, Y.; Harniman, R.; Winnik, M. A.; Manners, I. Hierarchical Assembly of Cylindrical Block Comicelles Mediated by Spatially Confined Hydrogen-Bonding Interactions. *J. Am. Chem. Soc.* **2016**, *138*, 12902-12912.

(14) Li, X. Y.; Gao, Y.; Boott, C. E.; Hayward, D. W.; Harniman, R.; Whittell, G. R.; Richardson, R. M.; Winnik, M. A.; Manners, I. “Cross” Supermicelles via the Hierarchical

Assembly of Amphiphilic Cylindrical Triblock Comicelles. *J. Am. Chem. Soc.* **2016**, *138*, 4087-4095.

(15) Wang, H.; Wang, X. S.; Winnik, M. A.; Manners, I. Redox-Mediated Synthesis and Encapsulation of Inorganic Nanoparticles in Shell-Cross-Linked Cylindrical Polyferrocenylsilane Block Copolymer Micelles. *J. Am. Chem. Soc.* **2008**, *130*, 12921-12930.

(16) Wang, H.; Patil, A. J.; Liu, K.; Petrov, S.; Mann, S.; Winnik, M. A.; Manners, I. Fabrication of Continuous and Segmented Polymer/Metal Oxide Nanowires Using Cylindrical Micelles and Block Comicelles as Templates. *Adv. Mater.* **2009**, *21*, 1805- 1808.

(17) Gädt, T.; Schacher, F. H.; McGrath, N.; Winnik, M. A.; Manners, I. Probing the Scope of Crystallization-Driven Living Self-Assembly: Studies of Diblock Copolymer Micelles with a Polyisoprene Corona and a Crystalline Poly(ferrocenyldiethylsilane) Core-Forming Metalloblock. *Macromolecules* **2011**, *44*, 3777-3786.

(18) Nazemi, A.; He, X.; MacFarlane, L. R.; Harniman, R. L.; Hsiao, M. S.; Winnik, M. A.; Faul, C. F. J.; Manners, I. Uniform "Patchy" Platelets by Seeded Heteroepitaxial Growth of Crystallizable Polymer Blends in Two Dimensions. *J. Am. Chem. Soc.* **2017**, *139*, 4409-4417.

(19) Gadt, T.; Ieong, N. S.; Cambridge, G.; Winnik, M. A.; Manners, I. Complex and Hierarchical Micelle Architectures from Diblock Copolymers using Living, Crystallization-Driven Polymerizations. *Nat. Mater.* **2009**, *8*, 144-150.

(20) Lotz, B.; Kovacs, A. J.; Bassett, G. A.; Keller, A. Properties of Copolymers Composed of One Poly(ethylene oxide) and One Polystyrene Block. *Kolloid- Zeitschrift und Zeitschrift für Polymere* **1966**, *209*, 115-128.

(21) Gast, A. P.; Vinson, P. K.; Cogan-Farinas, K. A. An Intriguing Morphology in Crystallizable Block Copolymers. *Macromolecules* **1993**, *26*, 1774-1776.

(22) Lazzari, M.; Scalarone, D.; Vazquez-Vazquez, C.; López-Quintela, M. A. Cylindrical Micelles from the Self-Assembly of Polyacrylonitrile-Based Diblock Copolymers in Nonpolar Selective Solvents. *Macromol. Rapid Commun.* **2008**, *29*, 352-357.

(23) He, W. N.; Zhou, B.; Xu, J. T.; Du, B. Y.; Fan, Z. Q. Two Growth Modes of Semicrystalline Cylindrical Poly(ε-caprolactone)-*b*-Poly(ethylene oxide) Micelles. *Macromolecules* **2012**, *45*, 9768-9778.

(24) Sun, J. R.; Chen, X. S.; He, C. L.; Jing, X. B. Morphology and Structure of Single Crystals of Poly(ethylene glycol)-Poly(ε-caprolactone) Diblock Copolymers. *Macromolecules* **2006**, *39*, 3717-3719.

(25) Su, M.; Huang, H.; Ma, X.; Wang, Q.; Su, Z. Poly(2-vinylpyridine)-*block*-Poly(ε-caprolactone) Single Crystals in Micellar Solution. *Macromol. Rapid Commun.* **2013**, *34*, 1067-1071.

(26) Du, Z. X.; Xu, J. T.; Fan, Z. Q. Micellar Morphologies of Poly(ε-caprolactone)-*b*-Poly(ethylene oxide) Block Copolymers in Water with a Crystalline Core. *Macromolecules* **2007**, *40*, 7633-7637.

(27) Yang, J. X.; Fan, B.; Li, J. H.; Xu, J. T.; Du, B. Y.; Fan, Z. Q. Hydrogen-Bonding-Mediated Fragmentation and Reversible Self-assembly of Crystalline Micelles of Block Copolymer. *Macromolecules* **2016**, *49*, 367-372.

(28) Petzetakis, N.; Dove, A. P.; O'Reilly, R. K. Cylindrical Micelles from the Living

Crystallization-Driven Self-Assembly of Poly(lactide)-Containing Block Copolymers. *Chem. Sci.* **2011**, *2*, 955-960.

(29) Petzetakis, N.; Walker, D.; Dove, A. P.; O'Reilly, R. K. Crystallization-Driven Sphere-to-Rod Transition of Poly(lactide)-*b*-Poly(acrylic acid) Diblock Copolymers: Mechanism and Kinetics. *Soft Matter* **2012**, *8*, 7408-7414.

(30) Sun, L.; Petzetakis, N.; Pitto-Barry, A.; Schiller, T. L.; Kirby, N.; Keddie, D. J.; Boyd, B. J.; O'Reilly, R. K.; Dove, A. P. Tuning the Size of Cylindrical Micelles from Poly(L-lactide)-*b*-Poly(acrylic acid) Diblock Copolymers Based on Crystallization-Driven Self-Assembly. *Macromolecules* **2013**, *46*, 9074-9082.

(31) Pitto-Barry, A.; Kirby, N.; Dove, A. P.; O'Reilly, R. K. Expanding the Scope of the Crystallization-Driven Self-Assembly of Polylactide-Containing Polymers. *Polym. Chem.* **2014**, *5*, 1427-1436.

(32) Sun, L.; Pitto-Barry, A.; Kirby, N.; Schiller, T. L.; Sanchez, A. M.; Dyson, M. A.; Sloan, J.; Wilson, N. R.; O'Reilly, R. K.; Dove, A. P. Structural Reorganization of Cylindrical Nanoparticles Triggered by Polylactide Stereocomplexation. *Nat. Commun.* **2014**, *5*, 5746.

(33) Inam, M.; Cambridge, G.; Pitto-Barry, A.; Laker, Z. P. L.; Wilson, N. R.; Mathers, R. T.; Dove, A. P.; O'Reilly, R. K. 1D *vs*. 2D Shape Selectivity in the Crystallization-Driven Self-Assembly of Polylactide Block Copolymers. *Chem. Sci.* **2017**, *8*, 4223-4230.

(34) Song, Y.; Chen, Y.; Su, L.; Li, R.; Letteri, R. A.; Wooley, K. L. Crystallization-Driven Assembly of Fully Degradable, Natural Product-Based Poly(L-lactide)-*block*-Poly(α-D-glucose carbonate)s in Aqueous Solution. *Polymer* **2017**, *122*, 270-279.

(35) Patra, S. K.; Ahmed, R.; Whittell, G. R.; Lunn, D. J.; Dunphy, E. L.; Winnik, M. A.; Manners, I. Cylindrical Micelles of Controlled Length with a π-Conjugated Polythiophene Core via Crystallization-Driven Self-Assembly. *J. Am. Chem. Soc.* **2011**, *133*, 8842-8845.

(36) Qian, J. S.; Li, X. Y.; Lunn, D. J.; Gwyther, J.; Hudson, Z. M.; Kynaston, E.; Rupar, P. A.; Winnik, M. A.; Manners, I. Uniform, High Aspect Ratio Fiber-like Micelles and Block Co-micelles with a Crystalline π-Conjugated Polythiophene Core by Self-Seeding. *J. Am. Chem. Soc.* **2014**, *136*, 4121-4124.

(37) Li, X. Y.; Wolanin, P. J.; MacFarlane, L. R.; Harniman, R. L.; Qian, J.; Gould, O. E. C.; Dane, T. G.; Rudin, J.; Cryan, M. J.; Schmaltz, T.; Frauenrath, H.; Winnik, M. A.; Faul, C. F. J.; Manners, I. Uniform Electroactive Fibre-like Micelle Nanowires for Organic Electronics. *Nat. Commun.* **2017**, *8*, 15909.

(38) Yu, B.; Jiang, X. S.; Yin, J. Multiresponsive Square Hybrid Nanosheets of POSS-Ended Hyperbranched Poly(ether amine) (hPEA). *Macromolecules* **2012**, *45*, 7135- 7142.

(39) Yu, B.; Jiang, X. S.; Yin, J. Size-Tunable Nanosheets by the Crystallization-Driven 2D Self-Assembly of Hyperbranched Poly(ether amine) (hPEA). *Macromolecules* **2014**, *47*, 4761-4768.

(40) Schmelz, J.; Schedl, A. E.; Steinlein, C.; Manners, I.; Schmalz, H. Length Control and Block-Type Architectures in Worm-like Micelles with Polyethylene Cores. *J. Am. Chem. Soc.* **2012**, *134*, 14217-14225.

(41) Schmelz, J.; Karg, M.; Hellweg, T.; Schmalz, H. General Pathway toward Crystalline-Core Micelles with Tunable Morphology and Corona Segregation. *ACS Nano* **2011**, *5*, 9523-9534.

(42) Schmelz, J.; Schacher, F. H.; Schmalz, H. Cylindrical Crystalline-Core Micelles: Pushing the Limits of Solution Self-Assembly. *Soft Matter* **2013**, *9*, 2101-2107.

(43) Lin, E. K.; Gast, A. P. Semicrystalline Diblock Copolymer Platelets in Dilute Solution. *Macromolecules* **1996**, *29*, 4432-4441.

(44) Li, Z.; Liu, R.; Mai, B.; Wang, W.; Wu, Q.; Liang, G.; Gao, H.; Zhu, F. Temperature-Induced and Crystallization-Driven Self-Assembly of Polyethylene-*b*-Poly(ethylene oxide) in Solution. *Polymer* **2013**, *54*, 1663-1670.

(45) Yin, L.; Hillmyer, M. A. Disklike Micelles in Water from Polyethylene-Containing Diblock Copolymers. *Macromolecules* **2011**, *44*, 3021-3028.

(46) Yin, L.; Lodge, T. P.; Hillmyer, M. A. A Stepwise "Micellization-Crystallization" Route to Oblate Ellipsoidal, Cylindrical, and Bilayer Micelles with Polyethylene Cores in Water. *Macromolecules* **2012**, *45*, 9460-9467.

(47) Fan, B.; Wang, R. Y.; Wang, X. Y.; Xu, J. T.; Du, B. Y.; Fan, Z. Q. Crystallization-Driven Co-Assembly of Micrometric Polymer Hybrid Single Crystals and Nanometric Crystalline Micelles. *Macromolecules* **2017**, *50*, 2006-2015.

(48) Blundell, D. J.; Keller, A.; Kovacs, A. J. A New Self-Nucleation Phenomenon and Its Application to the Growing of Polymer Crystals from Solution. *J. Polym. Sci. Polym. Lett.* **1966**, *4*, 481-486.

(49) Hsiao, M. S.; Chen, W. Y.; Zheng, J. X.; Van Horn, R. M.; Quirk, R. P.; Ivanov, D. A.; Thomas, E. L.; Lotz, B.; Cheng, S. Z. D. Poly(ethylene oxide) Crystallization within a One-Dimensional Defect-Free Confinement on the Nanoscale. *Macromolecules* **2008**, *41*, 4794-4801.

(50) Hsiao, M. S.; Zheng, J. X.; Van Horn, R. M.; Quirk, R. P.; Thomas, E. L.; Chen, H. L.; Lotz, B.; Cheng, S. Z. D. Poly(ethylene oxide) Crystal Orientation Change under 1D Nanoscale Confinement using Polystyrene-*block*-Poly(ethylene oxide) Copolymers: Confined Dimension and Reduced Tethering Density Effects. *Macromolecules* **2009**, *42*, 8343-8352.

(51) Li, B.; Li, C. Y. Immobilizing Au Nanoparticles with Polymer Single Crystals, Patterning and Asymmetric Functionalization. *J. Am. Chem. Soc*. **2007**, *129*, 12-13.

(52) Li, B.; Ni, C.; Li, C. Y. Poly(ethylene oxide) Single Crystals as Templates for Au Nanoparticle Patterning and Asymmetrical Functionalization. *Macromolecules* **2008**, *41*, 149-155.

(53) Li, X. Y.; Jin, B. X.; Gao, Y.; Hayward, D. W.; Winnik, M. A.; Luo, Y. J.; Manners, I. Monodisperse Cylindrical Micelles of Controlled Length with a Liquid-Crystalline Perfluorinated Core by 1D "Self-Seeding". *Angew. Chem., Int. Ed.* **2016**, *55*, 11392-11396.

(54) Tao, D. L.; Feng, C.; Cui, Y. N.; Yang, X.; Manners, I.; Winnik, M. A.; Huang, X. Y. Monodisperse Fiber-like Micelles of Controlled Length and Composition with an Oligo(*p*-phenylenevinylene) Core via "Living" Crystallization-Driven Self-Assembly. *J. Am. Chem. Soc*. **2017**, *139*, 7136-7139.

(55) Feng, C.; Jose Gonzalez-Alvarez, M.; Song, Y.; Li, I.; Zhao, G. Y.; Molev, G.; Guerin, G.; Walker, G.; Scholes, G. D.; Manners, I.; Winnik, M. A. Synthesis, Self-Assembly and Photophysical Properties of Oligo(2,5-dihexyloxy-1,4-phenylene vinylene)-*block*-Poly(ethylene glycol). *Soft Matter* **2014**, *10*, 8875-8887.

(56) Guerin, G.; Rupar, P.; Molev, G.; Manners, I.; Jinnai, H.; Winnik, M. A. Lateral Growth of

1D Core-Crystalline Micelles upon Annealing in Solution. *Macromolecules* **2016**, *49*, 7004-7014.

(57) Gonzalez-Alvarez, M. J.; Jia, L.; Guerin, G.; Kim, K. S.; Du, V. A.; Walker, G.; Manners, I.; Winnik, M. A. How a Small Modification of the Corona-Forming Block Redirects the Self-Assembly of Crystalline-Coil Block Copolymers in Solution. *Macromolecules* **2016**, *49*, 7975-7984.

(58) Zhang, M.; Rupar, P. A.; Feng, C.; Lin, K.; Lunn, D. J.; Oliver, A.; Nunns, A.; Whittell, G. R.; Manners, I.; Winnik, M. A. Modular Synthesis of Polyferrocenylsilane Block Copolymers by Cu-Catalyzed Alkyne/Azide "Click" Reactions. *Macromolecules* **2013**, *46*, 1296-1304.

(59) Lorenzo, A. T.; Arnal, M. L.; Sánchez, J. J.; Müller, A. J. Effect of Annealing Time on the Self-Nucleation Behavior of Semicrystalline Polymers. *J. Polym. Sci. Polym. Phys.* **2006**, *44*, 1738-1750.

(60) Massa, M. V.; Lee, M. S. M.; Dalnoki-Veress, K. Crystal Nucleation of Polymers Confined to Droplets: Memory Effects. *J. Polym. Sci. Polym. Phys*. **2005**, *43*, 3438- 3443.

(61) Maus, A.; Hempel, E.; Thurn-Albrecht, T.; Saalwächter, K. Memory Effect in Isothermal Crystallization of Syndiotactic Polypropylene --Role of Melt Structure and Dynamics? *Eur. Phys. J. E* **2007**, *23*, 91-101.

(62) Cossiello, R. F.; Susman, M. D.; Aramendía, P. F.; Atvars, T. D. Z. Study of Solvent-Conjugated Polymer Interactions by Polarized Spectroscopy: MEH–PPV and Poly(9,9′-dioctylfluorene-2,7-diyl). *J. Lumin.* **2010**, *130*, 415-423.

(63)Yagi, Y.; Inomata, H.; Saito, S. Solubility parameter of an N-isopropylacrylamide gel.

Macromolecules **1992**, *25*, 2997-2998.

(64) Topaloğlu Yazıcı, D.; Aşkın, A.; Bütün, V. GC Investigation of the Solubility Parameters of Water-Soluble Homopolymers and Double-Hydrophilic Diblock Copolymers. *Chromatographia* **2008**, *67*, 741-747.

Table of Contents

Self-Seeding of Block Copolymers with a π-Conjugated Oligo(*p*-phenylene vinylene) Segment: A Versatile Route toward Monodisperse Fiber-like Nanostructures

Daliao Tao,[a] *Chun Feng*,[a,*] *Yijie Lu*,[b] *Yinan Cui*,[a] *Xian Yang*,[a] *Ian Manners*,[c] *Mitchell A. Winnik*,[b,*] *Xiaoyu Huang*[a,*]